A Simple Approach for Mapping CSF Volume Fraction

Q. Qin[1], and P. C. van Zijl[1]
[1]Department of Radiology and Radiological Science, Johns Hopkins University, Baltimore, MD, United States

INTRODUCTION: Cerebrospinal fluid (CSF) is important for the hydrodynamic function of the central nervous system. Although long considered as just a partial volume confounder in functional MRI (fMRI), recently a more active role in fMRI contrast mechanism is being investigated for CSF: namely, redistribution in response to local blood volume changes during activation (1,2). As a consequence, mapping of volume fraction of CSF (VCSF) at baseline should benefit future studies on this matter. MRI methods to determine tissue composition are traditionally based on either fitting multi-compartment T_2 decay (3,4) or segmenting high-resolution T_1-weighted images (5,6). These methods, along with some newer techniques (7-9), all require long time for both acquisition and analysis. Coregistration of segmented high-resolution data to lower-resolution images acquired in fMRI also increases computational demand and prevents its routine use. By taking advantage of the much longer T_2 of CSF, here we propose a simple approach for mapping CSF volume using single-compartment T_2 decay model with only two parameters to fit in each voxel (VCSF and $T_{2,CSF}$).

METHODS: At 3T, most tissue T_2s are less than 120ms, except for CSF, which is longer than 1000ms. With a series of TEs all larger than 600ms, monoexponential signal decay, $S(TE)= S(0)\bullet\exp(-TE/T_{2,CSF})$, from pure CSF components can be isolated and magnetization at TE=0, $(S(0)=A\bullet VCSF\bullet(1-\exp(-TR/T_{1,CSF})))$, can thus be extrapolated. A is the signal equilibrium in a voxel containing pure CSF. VCSF of each voxel can readily be calculated by $VCSF=S(0)/(A\bullet(1-\exp(-TR/T_{1,CSF})))$. Another important feature of CSF is its flow, which makes it prone to wash-in/wash-out effects. T_2 values of flowing spins are typically measured using a so-called T_2 preparation (10-12).

Experiments were performed on a 3T Philips Intera scanner using body coil transmit and 8-channel head coil receive. Six healthy subjects (32~45yrs) were enrolled with informed consent. Our pulse diagram for measuring CSF volume is shown in Fig. 1, which includes 3 blocks within each TR: non-selective (NS) T_2 prep, slice-selective (SS) excitation/acquisition and NS saturation with a delay. NS T_2 prep block: 90^o_x, $[90^o_x 180^o_y 90^o_x]_N$, $270^o_x 360^o_{-x}$ were chosen to compensate for B_0/B_1 inhomogeniety with an MLEV phase pattern (10). With constant inter-echo spacing τ_{cpmg}=150ms, N=[4,6,8,10,12,14,16] refocusing pulses generated 7 different TE_{prep} (from 600ms to 2400ms, ΔTE_{prep}=300ms). At the end of the T_2 prep block, the longitudinal magnetizations (Mz) of spins are weighted by their T_2 factors, $\exp(-TE_{prep}/T_2)$. The residual transverse magnetizations are then dephased by a spoiling gradient. SS excitation/acquisition: THK=5mm, FOV=240x240mm^2, matrix=64x64, resolution = 3.75x3.75mm^2, single-shot gradient echo EPI acquisition (TE=20ms), N_{ave}=4 for each TE_{prep}. NS saturation: an adiabatic saturation pulse (BIR-4 (13)) immediately resets all recovered Mz to zero. So that after a fixed time delay, T_{delay}=4s, Mz of CSF right before each T_2 prep block would not be affected by previous T_2 weighting. Total time≈$7(N_{TEprep})x4(N_{ave})x6s(T_{delay}+TE_{prep})$≈2.6min.

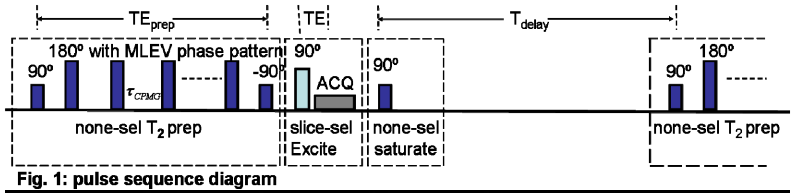

Fig. 1: pulse sequence diagram

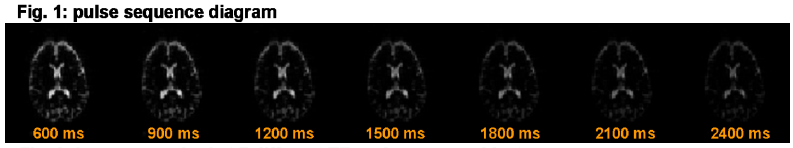

Fig. 2: Images acquired at 7 different TE_{prep} from one subject.

Signals at different TE_{prep} were fitted with monoexponential decay model using nonlinear-least-square algorithm. The goodness of fit was evaluated by R^2. When R^2>0.95, both CSF T_2 and S(0) were extracted. Then $VCSF=S(0)/(A\bullet(1-\exp(-T_{delay}/T_{1,CSF})))$ was calculated. The robustness of the technique was tested on one subject with the method proposed above and two modified schemes: 1): N=16 refocusing pulses in all 7 TE_{prep}; 2): T_{delay}=8s.

RESULTS AND DISCUSSION: Fig. 2 shows the images acquired at 7 different TE_{prep} from one subject. Fig. 3 displays maps of the CSF T_2, VCSF and goodness of fit R^2 respectively (Fig. 3a,b,c) with their corresponding histograms (Fig. 3d,e,f). It can be seen from the map of goodness of fit R^2 (Fig. 3c) that most voxels within cortex and ventricles suit well for the monoexponential decay model (R^2>0.97). Data within white matter deviate from this model mainly due to lack of long-T_2 signal (VCSF<0.03). The mean and SD of the CSF T_2 in voxels with valid fit is 1654ms±389ms for the same subject. This large range of measured T_2 might be caused by irreversible spin dephasing when CSF flows through inhomogeneous field during long inter-echo spacing τ_{cpmg}=150ms. VCSF in ventricles was close to 1 as expected and cortical CSF fraction ranged from 0.05 to 0.5 (Fig. 3b,e). Voxel-wise regression analysis of CSF volume measured using the proposed method and two modified schemes show excellent robustness: R^2>0.95 (Fig. 4).

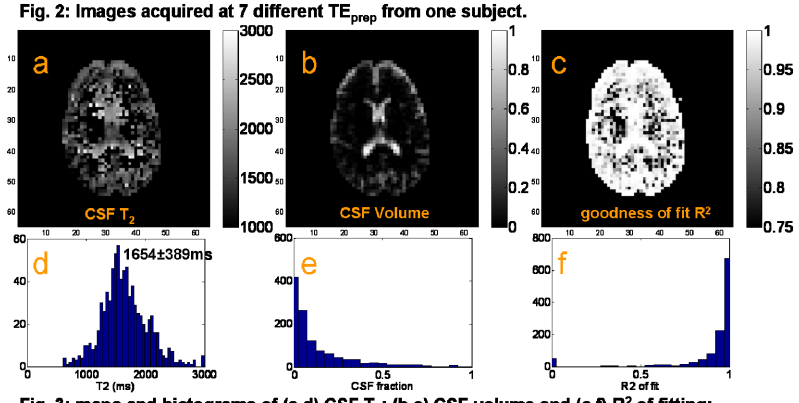

Fig. 3: maps and histograms of (a,d) CSF T_2; (b,e) CSF volume and (c,f) R^2 of fitting;

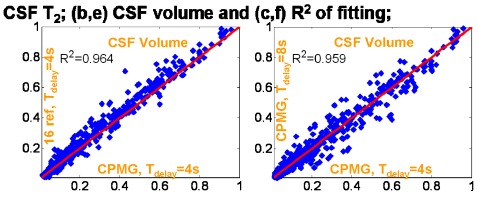

Fig. 4: Voxel-by-voxel regression plots of CSF volume measured using the proposed method (τ_{cpmg}=150ms, T_{delay}=4s) and two modified schemes. Left: 16 refocusing pulses in all TE_{prep}; Right: T_{delay}=8s.

CONCLUSION: A straightforward approach to quantify CSF volume in baseline was demonstrated that fits exponential decay of only CSF signal. The method should be easily expanded to 3D coverage due to long CSF T_2 and subsequently less signal decay during acquisition.

REFERENCE: 1. Scouten A, et al. *MRM* (2008) 58, p308; 2. Piechnik SK, et al. *MRM* (2009) 61, p579; 3. Ernst T, et al. *JMR B* (1993) 102, p1; 4. Whittall KP, et al. *MRM* (1997) 37, p34; 5. Ashburner J, et al. *Neuroimage* (1997) 6, p209; 6. Hethering HP, et al. *MRM* (1996) 36, p21; 7. Bonekamp D, et al. *MRM* (2005) 54, p1268; 8. He X, et al. *MRM* (2007) 57, p115; 9. Bender B, et al. *MRM* (2009) 61, p834; 10. Brittain JH, et al. *MRM* (1995) 33, p689; 11. Foltz WD, et al. *MRM* (1999) 42, p837; 12. Qin Q, et al. *ISMRM* (2009) 17, p3655; 13. Garwood M, et al. JMR (1991) 94, p511; Acknowledgement of grant resource: P41RR015241; RO1EB004130;